Ferric Chloride Etching of Low Carbon Steels

Richard B. Maynard, J. J. Moscony, and M. H. Saunders
Video Component and Display Division, Lancaster, PA 17604

Abstract—Beaker etching kinetics of low carbon steels (mainly 1008 rimmed steel) in ferric chloride-hydrochloric acid etchant are reported. A mechanism consisting of predominately transport-limited kinetics at low Baumé (~<40° Bé) and predominately surface-limited kinetics at high Baumé (~>54° Bé) is proposed. Activation parameters are: 32.0° Bé, $\Delta H^{\ddagger} = +3.07 \pm 0.13$ kcal/mole, $\Delta S^{\ddagger} = -25.3 \pm 0.3$ eu; 57.0° Bé, $\Delta H^{\ddagger} = +10.9 \pm 0.5$ kcal/mole, $\Delta S^{\ddagger} = -7.2 \pm 1.2$ eu. Chloride ion concentration was found to inhibit etch rate, particularly at high Baumé. Surface finish of etched pieces exhibit a transition Baumé region where surface roughness abruptly increases from ~6-7 microinches to well over 25 microinches. The transition Baumé region increases with an increase in temperature.

Introduction

The use of acidified ferric chloride solutions for etching metals is a widely utilized industrial process for producing burr-free precision piece-parts. In addition, it is one of several etchants utilized by the printed circuit industry in the production of printed and integrated circuit boards. Ferric chloride as an etchant is not only cheap and of low toxicity, but also reacts with a variety of metals and alloys. At RCA, it is currently utilized in the production of shadow masks for CRT devices from low carbon steels.

Recently we have become interested in the etching kinetics of ferric chloride with low carbon steels in the hope of gaining chemical insight into the mechanism and thermodynamic properties of this system. Our initial study focused on a simplified system using ferric perchlorate-perchloric acid as the etching medium.[1] This

etchant was utilized to simplify the number of ferric species present and to allow the reaction to be followed via UV spectrophotometry. From the results of that study, we postulated a mechanism consistent with an encounter-limited reaction rate between ferric ions and a steel substrate.

To model the actual process more precisely, we then substituted for the ferric perchlorate-perchloric acid etching medium a concentrated ferric chloride solution acidified with hydrochloric acid. In this paper we describe results of beaker etching low carbon steels (mainly 1008 rimmed steel) with ferric chloride etchant as a function of etchant concentration, temperature, and added chloride ions.

Experiment

Rectangular pieces of various steels measuring 36 × 52 mm were used. All were 0.15 mm in thickness except the FS steel which was 0.10 mm thick. All were cleaned by soaking in hot caustic solution, thoroughly rinsed with deionized water, and dried. Ferric chloride concentration was obtained via measurement of etchant density utilizing hydrometers calibrated with the heavy Baumé scale. Both specific gravity and molar concentration of ferric chloride can be interpolated by reference to standard tables.

Stock solutions of ferric chloride etchant were obtained and analyzed for ferrous chloride, ferric chloride, and free acid concentration. Higher Baumés were obtained by boiling water off the stock etchant and lower Baumés prepared by appropriate dilution with hydrochloric acid and deionized water. Except where noted, free acid concentrations were adjusted to 0.040 M.

Viscosity measurements were performed with a Brookfield LVF Viscometer with a modified ultra-low viscosity adapter. The modified adapter contained a titanium insert with an internal diameter of 2.4 cm and a Teflon #1 LV spindle used in place of the ultra-low spindle. The modified adapter was calibrated with a Brookfield viscosity standard. All viscosity measurements were taken at a shear rate of 60 rpm with the scale covering a range of 0–50.5 centipoise.

The reaction apparatus consisted of a tall one-liter beaker contained in a Plexiglas-CPVC assembly. A grooved Plexiglas cover was fitted over the top of the beaker. The cover was drilled for a thermometer port and for a Teflon stirring-rod port. A piece of steel was attached via a slot in the Teflon stirring rod and connected to a variable speed stirring motor. The entire assembly was weighted and placed in a constant-temperature water bath controlled to ±0.05°C by a Tempette TE-7 heater controller.

In a typical experiment, a 0.5 liter solution of etchant was ther-

mally equilibrated to the desired temperature by stirring with a strip of Mylar attached to the Teflon stirring rod. Upon reaching constant temperature, the Mylar strip was replaced with a preweighed rectangular piece of steel. Depending on the temperature and Baumé, the steel was allowed to react until ~0.1–0.4 grams had etched away, a time generally in the range 2–6 minutes. Upon completion of an etch run, the steel sample was immediately rinsed with deionized water, dried and weighed. At least three pieces of steel were etched at each temperature and Baumé utilizing the same etchant sample. Stirring speed was maintained to ±1 rpm with a Power Instruments Model 1981-AM Digital Phototachometer. Surface roughness measurements were made on a Bendix Type QC profilometer. Baumé measurements were made with Baumé hydrometers calibrated to 0.1°.

Etch rates (g/cm^2-sec) were calculated from the weight of material etched away per apparent surface area of sample and reaction time. Heterogeneous rates (cm/sec) were determined by dividing etch rates by the specific gravity of the steel.

Results

Fig. 1 shows the average etch rates* for beaker etching 1008 rimmed steel at five temperatures covering the range 40–80°C (104–176°F) and degrees Baumé over the range 30–58. Standard deviations are generally on the order of 1–4% of the reported value for the curves over 40–70°C. However, at 80°C, standard deviations in excess of 10% were noted for many of the reported etch rates. This was mainly the result of an increase in experimental difficulties encountered at this temperature. As a result, the values contained in the 80° curve show considerably more scatter than those obtained at lower temperatures. Minor eccentricities in the stirring rod on the order of several millimeters appeared to have no discernable effect upon etch rate.

In separate experiments it was found that pieces of steel etched under identical conditions for different times (1–5 minutes) had nearly identical etch rates. No dependence of etch rate upon the order of samples etched during a kinetic experiment was noted.

A representative sample from each kinetic experiment was measured for surface roughness. The results covering the Baumés of interest are shown in Fig. 2. At each temperature a sharply defined transition from smooth (<10 microinches) to rough (>10 microinches) surface finish is observed. The transition Baumé at which

* Except where noted, all kinetic experiments utilized a stirring rate of 100 rpm.

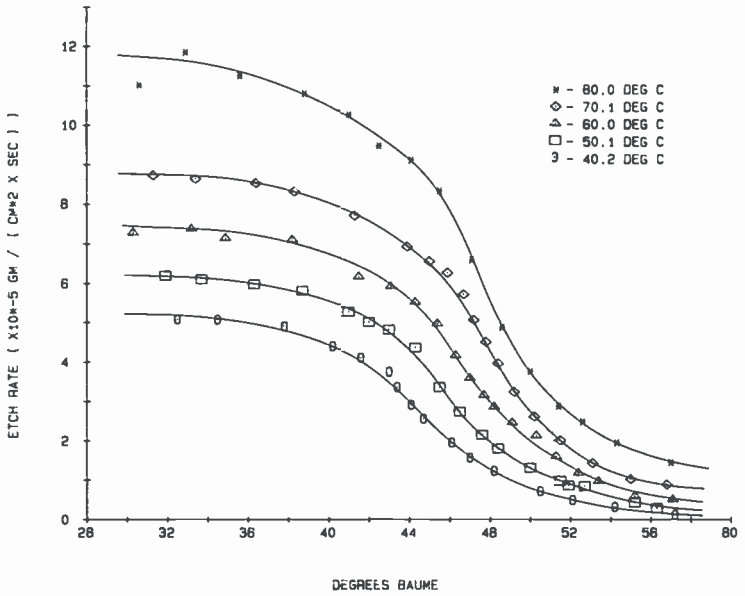

Fig. 1—Average etch rates (g/cm^2-sec) for 1008 rimmed steel as a function of Baumé and temperature.

this occurs is temperature dependent, increasing approximately one degree Baumé for every 10°C increase in temperature up to 70°C. Only a slight increase is then observed upon increasing the temperature from 70° to 80°C. Coincident with the increase in surface roughness is the appearance of smut upon the steel surface. The nonuniformity in the surface coverage by the smut is probably a contributing factor to the rough finish. Additionally, the roughness appears to increase with temperature.

From the temperature dependent data in Fig. 1, activation parameters were determined from heterogeneous rate constants obtained in the following manner. A "best-fit" curve was hand fitted to each temperature-dependent set of data points from 40.2° to 70.1°C in Fig. 1. Due to the scatter in the data points at 80.0°C these were not included in the calculation of activation parameters. The rate constants at 32.0° and 57.0° Bé were taken directly off each curve. Each rate constant was divided by the specific gravity of 1008 rimmed steel (7.87 g/cm^3) to give the heterogeneous rate constants contained in Table 1.

The effect[2] of absolute temperature T upon the heterogeneous rate k_h can be described by the empirical relation

$$k_h = A \exp\{-E_a/RT\} \qquad [1]$$

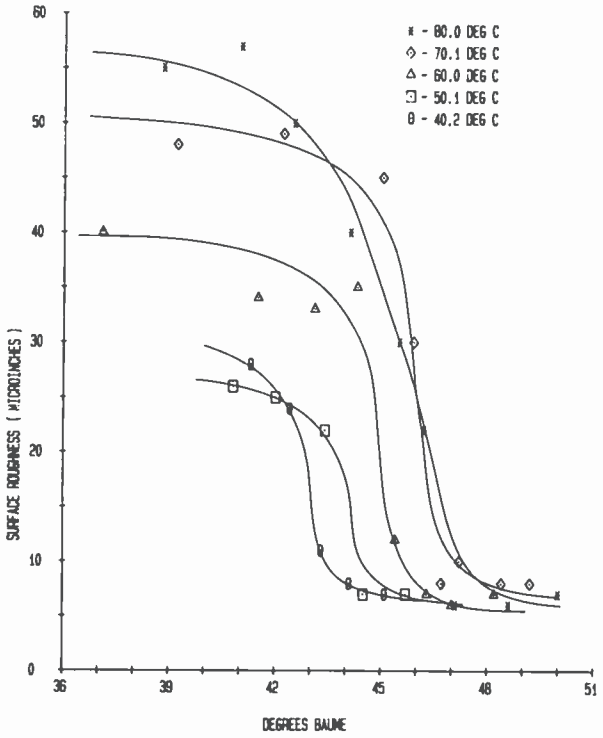

Fig. 2—Average surface roughness for 1008 rimmed steel as a function of Baumé and temperature.

where E_a is the activation energy and A the pre-exponential factor which is related to entropy. Since E_a and A are generally constant over a moderate temperature range, a plot of log k_h verus $1/T$ is linear with slope $-E_a/2.3R$ and intercept log A. An Arrhenius plot of 32.0° Bé is shown in Fig. 3 and activation energies obtained at 32.0° and 57.0° Bé are contained in Table 2.

Table 1—Observed Heterogeneous Rate Constant as a Function of Temperature for 1008 Rimmed Steel at a Stirring Rate of 100 RPM.

Temp (°K)	Observed Heterogeneous Rate Constant at 32.0° Bé ($\times 10^{-6}$ cm/sec)	Observed Heterogeneous Rate Constant at 57.0° Bé ($\times 10^{-7}$ cm/sec)
313.4 (40.2°C)	6.54	2.06
323.3 (50.1°C)	7.85	3.94
333.2 (60.0°C)	9.34	6.49
343.3 (70.1°C)	11.0	10.5

Table 2—Activation Parameters

Baumé	E_a kcal/mole	$\Delta H^{\ddagger}$ kcal/mole	$\Delta S^{\ddagger}$ (eu)
32.0°	+3.69 ± 0.12	+3.07 ± 0.13	−25.3 ± 0.3
57.0°	+11.5 ± 0.5	+10.9 ± 0.5	−7.2 ± 1.2

Alternatively, the free energy ($\Delta F^{\ddagger}$), enthalpy ($\Delta H^{\ddagger}$), and entropy ($\Delta S^{\ddagger}$) of activation can be obtained from the relation

$$k_h = \frac{KT}{h} \exp\left(\frac{-\Delta F^{\ddagger}}{RT}\right) = \frac{KT}{h} \exp\left(\frac{-\Delta H^{\ddagger}}{RT}\right) \exp\left(\frac{\Delta S^{\ddagger}}{R}\right) \qquad [2]$$

where K is Boltzmann's constant, h is Planck's constant, and T is absolute temperature. An Eyring plot of log (k_h/T) versus $1/T$ is linear with slope $-\Delta H^{\ddagger}/2.3R$ and intercept $\Delta S^{\ddagger}/2.3R$. Such a plot at 57.0° Bé is shown in Fig. 4. Enthalpy and entropy of activation energies at 32.0° and 57.0° Bé are tabulated in Table 2.

The effect of added chloride ions, as either hydrochloric acid or lithium chloride, was investigated and the results are given in Table 3. Three different Baumés were chosen as representative of the low, medium, and high Baumé regions. The resultant etch rates

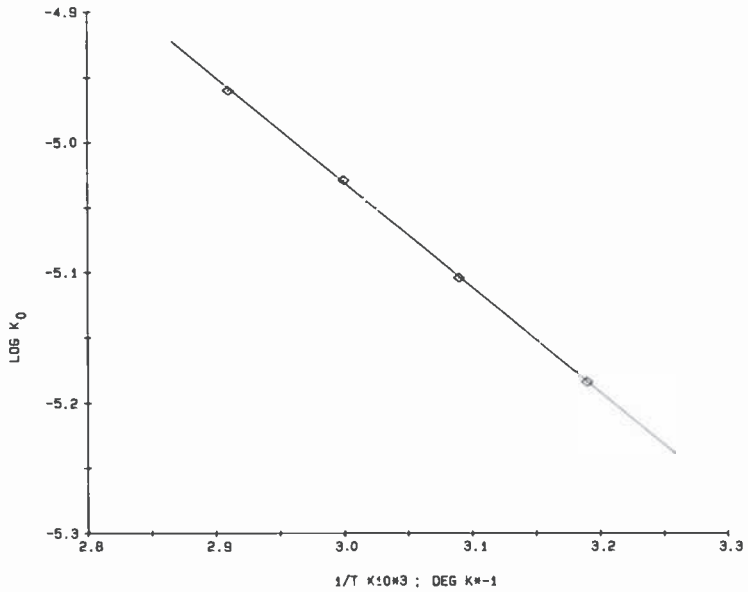

Fig. 3—An Arrhenius plot of log k versus $1/T$ (°K) at 32.0° Baumé for 1008 rimmed steel.

Table 3—Etch Rates for 1008 Rimmed Steel at 50.1°C and 100 RPM (Initial Free Acid Concentration 0.010 M)

Added HCl (M)	Added LiCl (M)	Baumé	Etch Rate ($\times 10^{-5}$ g/cm^2-sec)	% Change from Standard Etch-Rate Curve
		Low Baumé Region		
0.23		40.7	5.27 ± 0.13	−1.3
	0.23	40.8	5.21 ± 0.14	−1.9
0.46		39.9	5.41 ± 0.13	−2.2
	0.46	40.0	5.25 ± 0.10	−4.7
		Medium Baumé Region		
0.012		47.3	2.34 ± 0.02	+1.3
	0.012	47.4	2.29 ± 0.06	+1.5
0.058		47.5	2.28 ± 0.04	+3.6
	0.058	47.5	2.25 ± 0.01	+2.3
0.23		47.4	2.20 ± 0.01	−2.6
	0.23	47.6	2.13 ± 0.04	−0.9
0.46		46.4	2.48 ± 0.02	−11.1
	0.46	46.5	2.45 ± 0.02	−10.6
		High Baumé Region		
0.053		53.7	0.688 ± 0.006	+1.3
	0.053	53.3	0.764 ± 0.017	+2.7
0.11		53.7	0.621 ± 0.004	−8.5
	0.11	54.0	0.568 ± 0.007	−9.8
0.21		54.5	0.484 ± 0.012	−14.4
	0.21	54.4	0.461 ± 0.008	−18.4

were then compared to corresponding etch rates at the same Baumé obtained from the data in Fig. 1.

Upon examination of the results in Table 3 two trends become evident. First, the etch rate at a particular Baumé is dependent upon added chloride ion concentration irrespective of whether it is added as hydrochloric acid or lithium chloride. This appears to indicate that etch-rate depression is not a function of free-acid concentration. Apparently, the only role free-acid concentration plays is to insure a low pH to prevent ferric hydrolysis and the subsequent formation of solid iron hydroxides. Secondly, as the Baumé is increased, the concentration of added chloride ion necessary to decrease the etch rate decreases. For example, in the low Baumé region (40° Bé), an added chloride ion concentration of 0.46 M produces, at most, a slight etch-rate depression. However, in the high Baumé region (54° Bé), an added chloride ion concentration of 0.11 M decreases the etch rate approximately 10%. Further reductions are noted at higher chloride ion concentrations.

Besides 1008 rimmed steel, several other low carbon steels were briefly investigated. Table 4 gives the heterogeneous etch rates for five other low carbon steels etched in ferric chloride under similar

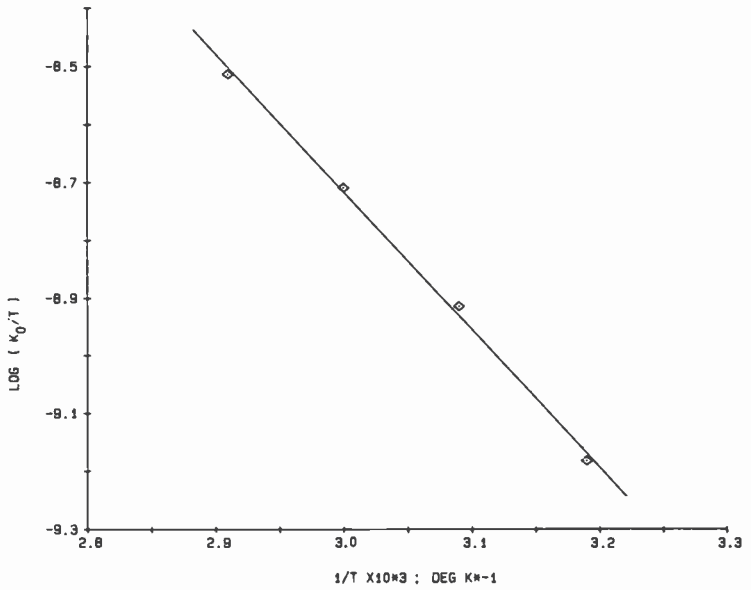

Fig. 4—An Eyring plot of log (k/T) versus $1/T$ (°K) at 57.0° Baumé for 1008 rimmed steel.

conditions of Baumé and temperature. All five steels etched at approximately the same rate as 1008 rimmed steel.

The similarity in etching characteristics of low carbon steels is readily seen in Figs. 5 and 6. Shown in Fig. 5 are etch rates for two steels as a function of Baumé at 70.1°C. Within the accuracy of our experiments, the etch rates for both steels are identical. Fig. 6 shows surface roughness measurements as a function of Baumé at 70.1°C. As observed for 1008 rimmed steel, a sudden increase in surface roughness is observed for 1005AK steel. Both steels show this increase at approximately the same Baumé.

Table 4—Heterogeneous Etch Rates for Various Steels at 46.7° Bé and 70.1°C

Steel	Heterogeneous Etch Rate[a] ($\times 10^{-6}$ cm/sec)
1008 rimmed	7.27 ± 0.25
1005AK	7.19 ± 0.10
1001AK	7.37 ± 0.17
FS[b]	6.78 ± 0.17
ARMCO-IF	6.85 ± 0.21
AK-AOD	7.27 ± 0.22

[a] stirring speed = 100 rpm
[b] 4 mils thick

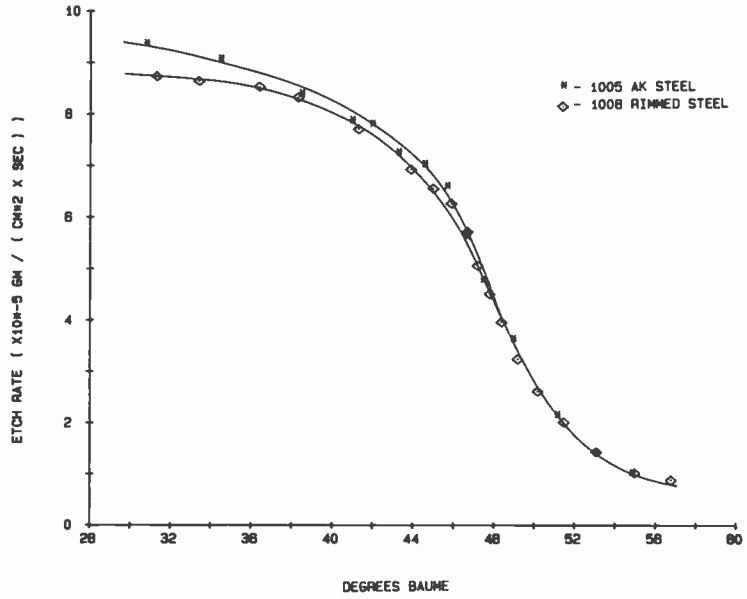

Fig. 5—Average etch rates (g/cm^2-sec) for 1005AK and 1008 rimmed steel as a function of Baumé at 70.1°C.

In addition to etch rates, we were also interested in the variation of viscosity of the etchant as a function of Baumé and temperature. These results are summarized in Fig. 7. As expected, the viscosity of the etchant increased as the Baumé increased. This results from the increase in dissolved material (ferric chloride) per unit volume which subsequently requires an increase in the force applied per unit area to maintain the same velocity gradient.[3]

Unexpected, however, was the appearance of a shoulder in the high Baumé region at high temperature. This gradually grew into a peak and shifted to a higher Baumé as the temperature decreased. Apparently a reorganization of the interactions between the ferric chloro species present and the solvent occurs over this particular Baumé region. We did observe, upon lowering the Baumé from ~60° through the region where the peak occurred, that more water than usual was required to produce the Baumé lowering. This suggests a change in the partial molar volume of the solvent resulting from a change in the solution structure. This could be the result of changes in the hydration sphere of a ferric chloro species which would alter the shape and/or size of the ferric chloro molecule. In turn, this would require the water molecules in the bulk solution to reorganize in order to accommodate this new species, producing the requisite change in partial molar volume.

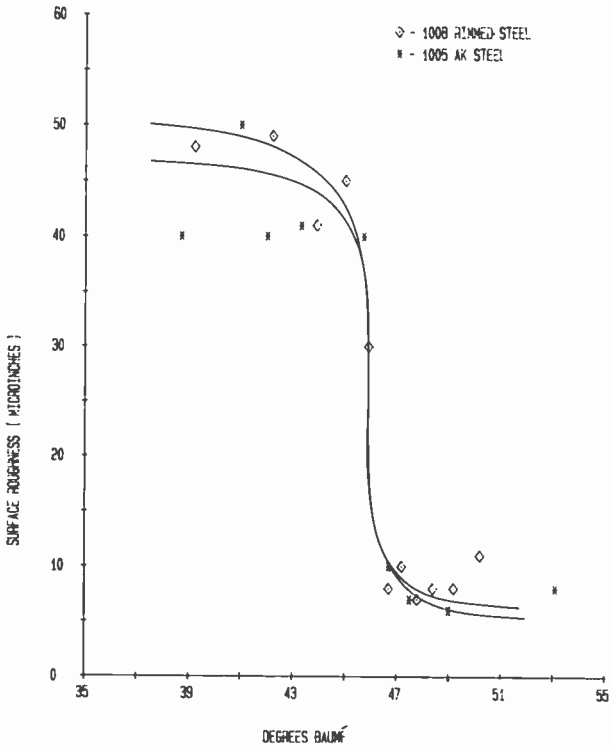

Fig. 6—Average surface roughness for 1005AK and 1008 rimmed steel as a function of Baumé at 70.1°C.

Discussion

The shape of the curves in Fig. 1 suggests to us a reaction where the mechanism is different at low and high Baumés. In these Baumé regions the etch rate changes very gradually, indicating the predominance of one mechanism over the other. Etch rates at intermediate Baumés are then composed of varying degrees of the two mechanisms producing a rapidly changing etch rate as Baumé is varied.

In the low Baumé region (32.0° Bé), an enthalpy of activation of $+3.07 \pm 0.13$ kcal/mole and an entropy of activation of -25.3 ± 0.3 were found. Diffusion of small molecules in solvents of low viscosity typically display enthalpy-of-activation values in the range $+1$ to 4 kcal/mole.[4] Also found in this Baumé region was a strong dependence of etch rate upon stirring (see Fig. 8) and surface area of the steel sample (see Table 5). These results suggest a reaction rate that is limited by the rate of encounter of ferric chloro species

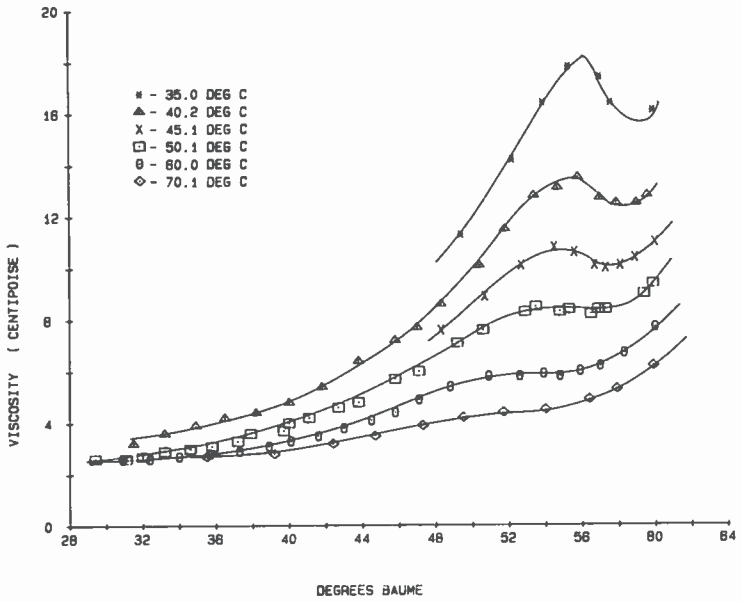

Fig. 7—Ferric Chloride viscosity (centipoise) as a function of Baumé and temperature.

with the steel substrate. Since the rate of encounter contains contributions from both mass transport and diffusion, we have, for convenience, followed the convention of others[5] and termed this rate-limiting process as "transport-limited" kinetics.

Additionally, the enthalpy and entropy of activation values are quite similar to those found for the ferric perchlorate-perchloric acid etch system described in Ref. [1]. In that system we observed transport-limited kinetics and proposed a mechanism involving transport of ferric ion from bulk solution to the steel surface as the rate determining step. On the basis of the above results, it appears highly

Table 5—Average Etch Rate as a Function of Steel Surface Area at 60.0°C (Stirring Rate = 100 RPM)

Surface Area (cm^2)	Average Etch Rate ($\times 10^{-5}$ g/cm^2-sec)
34.3° Bé	
28.1	7.94 ± 0.34
54.1	9.57 ± 0.10
55.9° Bé	
27.5	0.608 ± 0.009
54.4	0.620 ± 0.012

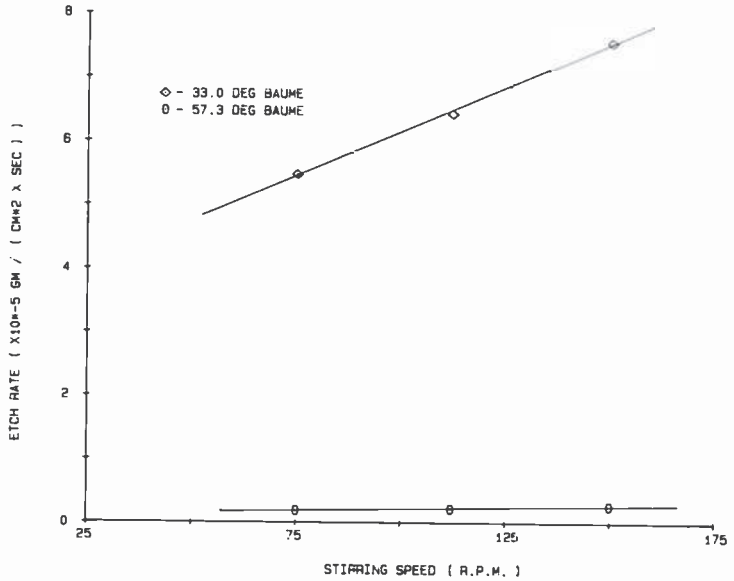

Fig. 8—Average etch rate (g/cm^2-sec) as a function of stirring speed at 33.0° and 57.3° Baumé at 50.1°C.

plausable to us that a similar rate-determining step involving ferric chloro specie(s) occurs in the low Baumé region.

In the high Baumé region, the kinetics are different from those observed in the low Baumé region. Unfortunately, the kinetic parameters for the high Baumé region could not be determined at a Baumé where the curves in Fig. 1 level out. This was due to the difficulty in keeping highly concentrated ferric chloride in solution. As a result, the kinetic results determined at 57.0° Bé do exhibit a slight contribution from the transport-limited kinetics occurring in the low Baumé region.

Nevertheless, an enthalpy of activation of $+10.9 \pm 0.5$ kcal/mole is too high for a diffusion controlled reaction. If diffusion is important, then the etchant viscosity should influence etch rate.[6] A comparison of etch rates at high Baumé (Fig. 1) with etchant viscosity (Fig. 7) indicates viscosity has a very limited effect upon etch rate, particularly at higher temperatures. If it did, then the shoulder observed in Fig. 7 should manifest itself in the etch rate curves. An examination of Fig. 1 reveals it does not. Instead, the enthalpy of activation falls into the range observed for processes dominated by adsorption. Energies of adsorption are generally in the range from about 9 to 100 kcal/mole.[7]

Further results reveal the etch rate to be virtually independent of stirring rate (Fig. 8)[8] and surface area of the steel sample (Table

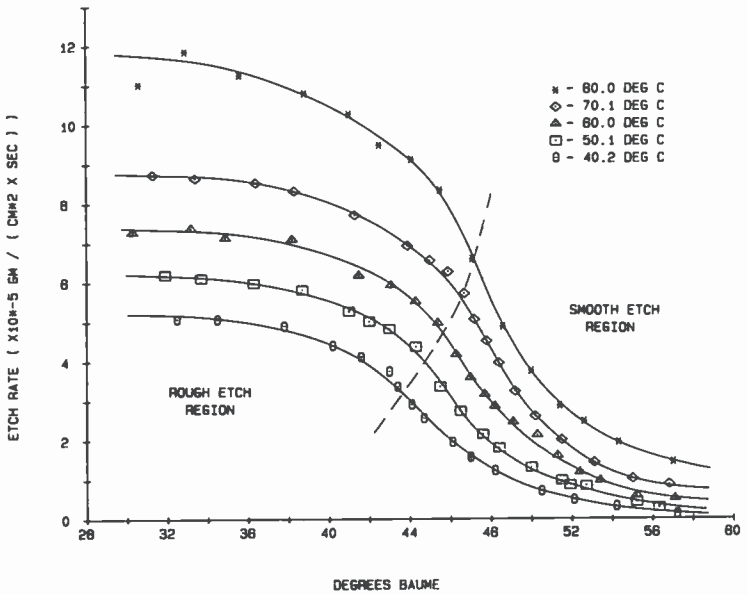

Fig. 9—Plot of Baumé and temperature combinations for smooth and rough etch.

5). All these results are consistent with reaction kinetics slower than transport limited and suggest to us a rate-limiting process involving surface reactions. This could involve adsorption of reactant, chemical reaction with surface iron atoms, desorption of products, or a combination of these processes. Since our present study doesn't allow us to choose which of the above processes are responsible for the rate-determining step, we have instead termed this rate-limiting process as "surface-limited" kinetics.

An apparent physical manifestation of the change in reaction mechanism from surface-limited kinetics to transport-limited kinetics is the sudden appearance of a nonuniform coating of smut on the surface of the etched pieces. This in turn, we believe, is responsible for the resultant increase in surface roughness seen in Fig. 2. Combining the results contained in Figs. 1 and 2 produces Fig. 9, which illustrates the various combinations of temperature and Baumé for obtaining either a smooth or rough surface finish.

The difference between a smooth and rough finish as the transition Baumé is passed is shown pictorially in the series of SEM topography photographs in Fig. 10. From top to bottom in the figure, an approximate six-fold increase in surface roughness is observed for a decrease of only 1.5° Bé. Knowledge of the transition Baumé could be important in etching, for example, the aperture openings in a shadow mask.

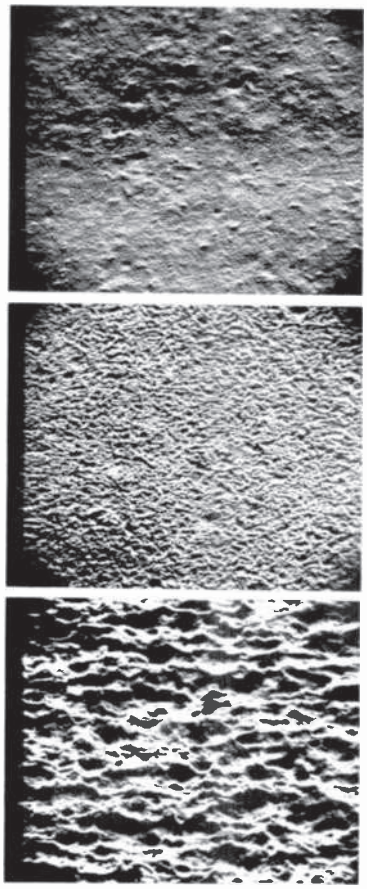

Fig. 10—SEM topography photographs of 1008 rimmed steel etched at 80°C. Sample surface roughness from top to bottom is, in microinches, 7 ± 1, 22 ± 2, and 45 ± 5. Original photos were at 500× 45° and have been reduced roughly by half here.

A possible explanation for the change in reaction mechanism as Baumé is varied involves a change in the identity of the reacting ferric chloro species. For example, upon increasing the Baumé at 25°C from 32° to 61° Bé, the ferric concentration increases from 2.3 to 6.8 M. Several different groups[9–11] utilizing Raman, ESR, and solution x-ray diffraction techniques upon concentrated ferric chloride solutions have shown that the identity of the ferric chloro species present changes over this concentration range. Although the identities of the ferric chloro species present at a particular concentration are interpreted somewhat differently by each group of workers, they do agree that increasing the ferric chloride concentration changes the principle species in solution.

From the results of the above-mentioned workers and considering equilibrium values[12,13] for the various ferric chloro species, it appears that three ferric chloro species are involved. In the low concentration range both $FeCl_2(H_2O)_4^{1+}$ and $FeCl_3(H_2O)_3$ are present, with the former probably in greater concentration than the latter. As the concentration (Baumé) increases, $FeCl_3(H_2O)_3$ becomes the predominate species with $FeCl_2(H_2O)_4^{1+}$ declining. At the same time $FeCl_4^{1-}$ starts appearing and at high concentrations becomes the predominate species. The appearance of $FeCl_4^{1-}$ is further enhanced by the presence of chlorides.[9]

Immediately apparent is the different charge associated with each of the ferric chloro species. Two of the ferric chloro species are ionic with charges of equal but opposite sign, and the other is nonionic. Also of importance is the presence or absence of the counter ion associated with each reacting species. Taken together, the various chemical species present in solution determine the adsorption characteristics of the electrical double layer between the steel substrate and bulk solution.[14] Changing the charge or eliminating it on the reacting species would be expected to have a profound effect upon the electrical double layer, resulting in a change in the rate of adsorption. If the presence of $FeCl_4^{1-}$ slows the rate of adsorption sufficiently, then a change in reaction mechanism from transport-limited to surface-limited would occur.

A result that supports this theory is the effect of added chloride ions upon etch rate. As shown in Table 3, added chloride ions cause a greater etch rate inhibition as the Baumé is increased. In the Baumé regions where $FeCl_4^{1-}$ formation is favored, adding excess chloride ions would greatly enhance $FeCl_4^{1-}$ formation. Any increase in $FeCl_4^{1-}$ concentration would then cause the observed reduction in etch rate.

Finally, it is of interest to compare our results with those of Allen and co-workers[15] who studied ferric chloride etching of annealed AISI 304 stainless steel. The etch rate versus Baumé (30°–45° Bé at 30° and 50°C) curves they generated were somewhat different than those in Fig. 1. They found that upon decreasing the Baumé, an increase in etch rate occurred until ~38°–42° Bé, where the etch rate leveled off before rising to a maximum at ~33–34° Bé. Our results also show an increase in etch rate as Baumé decreases, but we observed no inflexion point at ~38°–42° Bé. They ascribe this inflection point to a changeover in reaction mechanisms. The changeover is possibly due to the presence of significant alloying elements (19% Cr; 10% Ni) in the AISI 304 stainless steel.

The difference in surface roughness between the two steel types as Baumé and temperature are varied is even more striking. Instead

of the sudden increase in surface roughness observed with 1008 rimmed steel, they observed a smooth increase in surface roughness as Baumé was decreased. Interestingly, they found a greater increase in surface roughness at lower temperatures, whereas we observed this at higher temperatures. Again, this is probably due to differences in the chemical composition of the two steels.*

Both steels exhibit a similar decrease in etch rate as free acid is increased. Although Allen and his coworkers studied this only at 40.2° Bé (30° and 50°C), their results are in agreement with ours in this Baumé region. However, they also observed at this Baumé that the surface roughness could be drastically changed by varying free-acid concentration. In contrast, we found that 1008 rimmed steel shows no dependence of surface roughness upon free-acid concentration around the Baumé where the transition from smooth to rough surface finish occurs.

The point to be made from this comparison is that differences in steel composition due to significant amounts of alloying elements can drastically change the manner in which the material will etch in ferric chloride. Thus, conclusions concerning etch rate and surface finish based upon etching one type of material may not be applicable to a different untried material.

Conclusions

The etching dynamics of 1008 rimmed steel with ferric chloride consists of two competing reaction mechanisms. In the region of low Baumé ($\sim<40$ Bé) transport-limited kinetics dominate, while at high Baumé ($\sim>54°$ Bé) surface-limited kinetics dominate. Intermediate Baumés are a combination of varying degrees of the two types of reaction kinetics.

Surface finish of etched pieces is dependent upon Baumé and, to a lesser extent, upon temperature. A sudden increase in surface roughness is observed at a specific Baumé and temperature. Increasing the temperature of the etchant increases the Baumé where this is observed. Additionally, increased surface roughness may contribute to general nonuniformity in an etched piece.

High chloride ion concentrations were found to inhibit etch rates, particularly at high Baumés, and have no noticeable effect upon surface roughness.

* Allen et al (Ref. [15]) utilized spray etching. We do not believe this to be a major contributing factor in the differences observed between our study and theirs.

Acknowledgments

The authors wish to thank Dale Goodman for measuring surface roughness and JoAnn Wolfe for the SEM topography photographs.

References:

[1] R. B. Maynard, J. J. Moscony, and M. H. Saunders, "A Study of the Etching Kinetics of Low Carbon Steel Using the Ferric Perchlorate-Perchloric Acid System as a Model," *RCA Review*, **45**, p. 58, March 1984.
[2] R. G. Wilkins, *The Study of Kinetics and Mechanisms of Reactions of Transition Metal Complexes*, p. 79–81, Allyn and Bacon, Inc., Boston, MA, 1974.
[3] V. Fried, H. F. Hameka, and U. Blukis, *Physical Chemistry*, p. 64, McMillan Publishing Co., Inc., New York, 1977.
[4] S. W. Benson, *The Foundation of Chemical Kinetics*, p. 499, McGraw-Hill, New York, 1960; D. Shooter in *Comprehensive Chemical Kinetics*, Vol. 1, p. 253, C. H. Bamford and D. F. H. Tipper, Eds., Elsevier, Amsterdam, 1969.
[5] H. R. Rogers, C. L. Hill, Y. Fujiwara, R. J. Rogers, H. L. Mitchell, and G. M. Whitesides, "Mechanism of Formation of Grignard Reagents. Kinetics of Reaction of Alkyl Halides in Diethyl Ether with Magnesium," *J. Amer. Chem. Soc.*, **102**, p. 217, 1980.
[6] W. Jost, *Diffusion in Solids, Liquids and Gases*, p. 2, Academic Press, Inc., New York, 1952.
[7] W. J. Moore, *Physical Chemistry*, 4th Ed., p. 496, Prentice-Hall, Inc., Englewood Cliffs, NJ, 1972.
[8] V. Fried, H. F. Hameka and U. Blukis, *Physical Chemistry*, p. 710, McMillan Publishing Co., Inc., New York, 1977.
[9] W. L. Marston and S. F. Bush, "Raman Spectral Investigation of the Complex Species of Ferric Chloride in Concentrated Aqueous Solution," *Appl. Spectros.*, **26**, p. 579, 1972.
[10] M. Magini and T. Radnai, "X-Ray Diffraction Study of Ferric Chloride Solutions and Hydrated Melt. Analysis of the Iron(III)-Chloride Complexes Formation," *J. Chem. Phys.*, **71**, p. 4255, 1979; G. Giubileo, M. Magini, G. Licheri, G. Paschina, G. Piccaluga, and G. Pinna, "On the Structure of Iron(III) Chloride Solutions," *Inorg. Chem.*, **22**, p. 1001, 1983.
[11] D. L. Wertz and M. L. Steele, "Coordination of Fe^{3+} in Concentrated Aqueous Solutions with Chloride Ligands," *Inorg. Chem.*, **19**, p. 1652, 1980; D. L. Wertz and M. D. Luter, "Evolving Cation Coordination in Aqueous Solutions Prepared from Iron(III) Chloride Hexahydrate," *Inorg. Chem.*, **20**, p. 3118, 1981.
[12] G. A. Gamlen and D. O. Jordan, "A Spectroscopic Study of the Iron(III) Chloro-Complexes," *J. Chem. Soc.*, p. 1453, 1953.
[13] Y. Strahm, R. C. Patel and E. Matijevic, "Thermodynamics and Kinetics of Aqueous Iron(III) Chloride Complex Formation," *J. Phys. Chem.*, **83**, p. 1689, 1979.
[14] A. W. Adamson, *Physical Chemistry of Surfaces*, 3rd Ed., p. 411, John Wiley and Sons, New York, 1976; M. J. Rosen, *Surfactants and Interfacial Phenomena*, p. 26, John Wiley and Sons, New York, 1978.
[15] D. M. Allen, A. J. Hegarty and D. F. Horne, "Surface Textures of Annealed AISI 304 Stainless Steel Etched by Aqueous Ferric Chloride-Hydrochloric Acid Solutions," *Trans. Inst. Met. Finish*, **59**, p. 25, 1981.